

Unconstraining the Unhiggs

Christoph Englert,^{1,*} Michael Spannowsky,^{1,†} David Stancato,^{2,‡} and John Terning^{2,§}

¹*Institute for Particle Physics Phenomenology, Department of Physics, Durham University, Durham DH1 3LE, UK*

²*Department of Physics, University of California, Davis, CA 95616, USA*

We investigate whether or not perturbative unitarity is preserved in the Unhiggs model for the scattering process of heavy quarks and longitudinal gauge bosons $\bar{q}q \rightarrow V_L^+ V_L^-$. With the Yukawa coupling given in the original formulation of the Unhiggs model, the model preserves unitarity for Unhiggs scaling dimensions $d \leq 1.5$. We examine the LHC phenomenology that is implied by the Unhiggs model in this parameter range in detail and discuss to what extent the LHC can test d if an excess is measured in the phenomenologically clean ZZ channel in the future or if the LHC measurement remains consistent with the background. We then make use of the AdS/CFT correspondence to derive a new Yukawa coupling that is conformally invariant at high energies, and show that with this Yukawa coupling the theory is unitary for $1 \leq d < 2$.

I. INTRODUCTION

Georgi [1, 2], introduced a new approach to studying conformal sectors by specifying the two-point functions of scalar fields with a scaling dimension between one and two. Since the phase space for these fields resembles the phase space of a fractional number of particles, Georgi termed them “unparticles”. Subsequently, efforts were made to gauge unparticle actions in a consistent way [3] so that unparticles could be given Standard Model (SM) gauge quantum numbers. This also necessitates the introduction of an IR cutoff for the unparticle sector [3–5] so that there are no new massless modes, which would dramatically alter low energy phenomenology. Reference [6] introduced the Unhiggs as a way to break electroweak symmetry via an unparticle (see [7, 8] for work on related ideas). The Unhiggs has the same gauge structure as the SM Higgs with a scaling dimension d and an IR cutoff μ . The effects of an Unhiggs on precision electroweak measurements have been studied in detail [9, 10], and the model is consistent with the current data. In [6], it was demonstrated that like the SM Higgs, the Unhiggs unitarizes WW scattering and also that the Unhiggs can help ease the Little Hierarchy Problem. Reference [11] began to look into phenomenological aspects of the Unhiggs model, specifically the top quark decay $t \rightarrow W^+ b$. Due to the fact that the longitudinal W bosons are affected by the electroweak symmetry breaking sector, the fraction of emitted longitudinal W bosons is different in the Unhiggs model than it is in the SM. This information was used, along with CDF data and upcoming anticipated Large Hadron Collider (LHC) data, to put current and expected bounds on the (μ, d) parameter space in the Unhiggs model. In this paper we comment on the LHC phenomenology of the Unhiggs model in the parameter range $d \leq 1.5$ and return to a more theoretical aspect of the Unhiggs model, that of perturbative unitarity for $d > 1.5$.

We examine to what extent the Unhiggs can be constrained, ruled out or even measured statistically significant at the LHC if $d \leq 1.5$ in the heavy mass region. This is the mass range where Higgs decays in the SM are dominated by decays to massive gauge bosons. It is difficult to get around the current exclusion bounds [12] in this channel as a consequence of electroweak symmetry breaking [13], which guarantees $\Gamma(H \rightarrow ZZ) \sim m_H^3/m_Z^2$ for $m_H \gtrsim 2m_Z$. We will see that the Unhiggs model is an efficient realization of such a hiding mechanism, and from this point of view the Unhiggs phenomenology in the clean $ZZ \rightarrow 4\ell$ final state is especially interesting to reinterpret the current and future bounds on SM-like production [14–18].

For the parameter choice $d \leq 1.5$ we can expect a valid effective theory description by the Unhiggs model up to several TeV [6]. We will see that a non-observation of the Higgs boson can be consistently interpreted in this model. Increasing d beyond 1.5, we show that the Yukawa coupling in the original formulation of the Unhiggs [6], which explicitly breaks the conformal symmetry, is the root cause of unitarity violation in massive quark scattering $\bar{q}q \rightarrow W^+ W^-$. We show analytically that this “non-conformal” Yukawa coupling is not sufficient to preserve unitarity for values of the scaling dimension d greater than 1.5. To preserve unitarity, we need to derive a form of the Yukawa coupling which respects the conformal symmetry of the model. We accomplish this by appealing to the AdS/CFT correspondence [19], considering an AdS dual to the Unhiggs model. Once gauged, this “conformal” Yukawa coupling

*Electronic address: christoph.englert@durham.ac.uk

†Electronic address: michael.spannowsky@durham.ac.uk

‡Electronic address: dastancato@ucdavis.edu

§Electronic address: terning@physics.ucdavis.edu

will also necessitate the presence of terms in the Lagrangian with arbitrary numbers of gauge bosons. Taking these new terms into account, we find that unitarity is indeed preserved for all values of d in the range $1 \leq d < 2$.

II. MIXED YUKAWA-GAUGE SECTOR THEORY AND PHENOMENOLOGY

A. Remarks on perturbativity for $1 \leq d \leq 1.5$

We show first that the Yukawa coupling in [6] which is the most naive extension of the SM Yukawa coupling to an unparticle, is sufficient to preserve perturbative unitarity in the scattering process $\bar{t}t \rightarrow V_L V_L$ ($V = W^\pm, Z$). We will assume the scattering particles are top quarks, but the same general analysis follows for the other SM fermions as well. In the SM, there are four tree level diagrams contributing to $\bar{t}t \rightarrow W_L W_L$. These diagrams involve exchange of an s -channel photon, an s -channel Z boson, a t -channel bottom quark and an s -channel Higgs, and all have an analog in the Unhiggs model (see figures 1 and 2). The three diagrams in figure 1 that do not contain an Unhiggs have the same amplitude as in the Standard Model. This is obvious for the diagram with the t -channel bottom exchange because the bottom-top- W vertices as well as the bottom propagator are completely independent of the EWSB sector.

The s -channel photon and Z diagrams also yield the same amplitudes as in the SM, although it is not as obvious, because not only are their propagators different in the Unhiggs model, but there are additional vertices not present in the SM which would seem to contribute new diagrams to the scattering amplitude. First we will address the propagators. The photon and Z propagator in the Unhiggs model are both of the form

$$\Delta(q^2) = \frac{-i}{q^2 - M_Z^2} (g_{\mu\nu} - f(q^2)q^\mu q^\nu) \quad (1)$$

The function $f(q^2)$ is different for the photon and Z , and both are different from their counterparts in the SM. These functions are given in [6], but their actual form is unimportant because we will show that any term proportional to $q^\mu q^\nu$ in the propagator disappears in the amplitude for the s -channel exchange diagram. By contracting the second term in the propagator with the W^+W^-A or W^+W^-Z SM vertex and the polarization vectors, we find that both amplitudes are proportional to

$$\mathcal{M} \supset \mathcal{F}^\mu q_\mu q_\nu [(q + k^+)^\lambda g^{\nu\alpha} + (k^- - k^+)^\nu g^{\alpha\lambda} - (q + k^-)^\alpha g^{\nu\lambda}] \varepsilon_\lambda(k^-) \varepsilon_\alpha(k^+) \quad (2)$$

where $k^+(k^-)$ are the momenta of the $W^+(W^-)$ bosons, and F^μ is a Dirac chain representing the rest of the amplitude. Using $q = p + p' = (2E, 0, 0, 0)$, where p, p' are the quark momenta (*cf.* Fig. 1), we find that

$$q \cdot (k^- - k^+) = 0 \quad (3)$$

$$q \cdot \varepsilon(k^-) = 2E^2/M_W \quad (4)$$

$$q \cdot \varepsilon(k^+) = 2E^2/M_W \quad (5)$$

$$(q + k^+) \cdot \varepsilon(k^-) = 4E^2/M_W \quad (6)$$

$$(q + k^-) \cdot \varepsilon(k^+) = 4E^2/M_W. \quad (7)$$

Plugging in, this gives us $\mathcal{M} \sim E^4/M_W^2[8 + 0 - 8] = 0$. Thus, the part of the propagator proportional to $q_\mu q_\nu$ does not contribute to the amplitude and therefore the fact that the functions $f(q^2)$ are different in the Unhiggs model and the SM does not affect the amplitudes.

Next we must address the fact that there are new vertices in the Unhiggs model which naively contribute to the s -channel photon and Z amplitudes. Because of the non-local kinetic term in the Unhiggs model, there are vertices with two Unhiggs and arbitrary numbers of gauge bosons. Specifically there are W^+W^-AHH and W^+W^-ZHH vertices, and upon taking the Unhiggs to VEVs, these new three gauge boson vertices contribute to the amplitudes for the s -channel scattering processes. However, by using the method of gauging non-local Lagrangians given in [20], we find that these vertices contain only terms proportional either to k_μ^+ and/or k_ν^- . Upon contracting these vertices with the polarization vectors $\varepsilon_\mu(k^+)$ and $\varepsilon_\nu(k^-)$ the amplitude vanishes. Therefore, the amplitudes resulting from the three diagrams shown in figure 1 all take the same values as in the SM.

The results for these amplitudes in the SM are given in [21]. The cases where the top and anti-top have opposite helicities are not of interest because the Unhiggs exchange diagram is only non-zero when the helicities are either both right-handed or both left-handed. In other words, in the cases with opposite helicity, the three non-Higgs diagrams are all that is needed to preserve unitarity. In [21] it is indeed explicitly shown that these three diagrams conspire together to cancel all terms which are proportional to positive powers of the center of mass energy \sqrt{s} . As for the

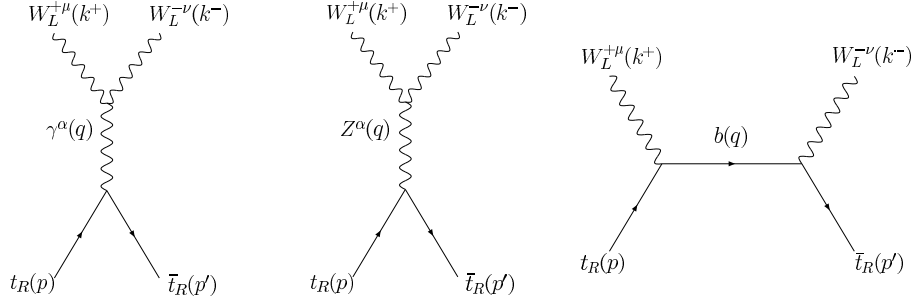
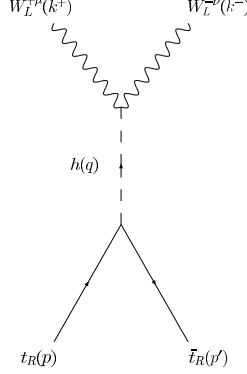


FIG. 1: The three diagrams not involving the Unhiggs.

FIG. 2: The s -channel Unhiggs exchange diagram.

cases where the helicities of the top and anti-top are the same, the results are also given in [21]. We will write the results for the top and anti-top having right-handed helicities here for future reference, keeping only the terms which grow with energy.

$$\mathcal{M}_{\gamma,RR} = 4\sqrt{2}G_F \left(\frac{2}{3}\right) m_t s_w^2 \cos\theta \sqrt{s} \quad (8)$$

$$\mathcal{M}_{Z,RR} = \sqrt{2}G_F m_t \left[4 \left(\frac{2}{3}\right) s_w^2 - 1\right] \cos\theta \sqrt{s} \quad (9)$$

$$\mathcal{M}_{b,RR} = \sqrt{2}G_F m_t (1 - \cos\theta) \sqrt{s} \quad (10)$$

where θ is the angle between the outgoing top quark and W_L^- . Adding these three contributions, we get

$$\mathcal{M}_{\gamma+Z+b,RR} = \sqrt{2}G_F m_t \sqrt{s}. \quad (11)$$

In the Standard Model, the s -channel Higgs exchange diagram is given by

$$\mathcal{M}_{H,RR} = -\sqrt{2}G_F m_t \sqrt{s}. \quad (12)$$

The cases with both particles left-handed is identical other than an opposite overall sign. We will therefore consider only the right-handed case for the rest of the paper with no loss of generality. Clearly in the SM the terms which grow with energy cancel once the Higgs exchange is included.

The Unhiggs exchange diagram

We now show that the Unhiggs exchange diagram in figure 2, using the naive “non-conformal” Yukawa coupling from [6], is not sufficient to preserve unitarity for the entire range of d , $1 \leq d < 2$. The Yukawa term in the Lagrangian

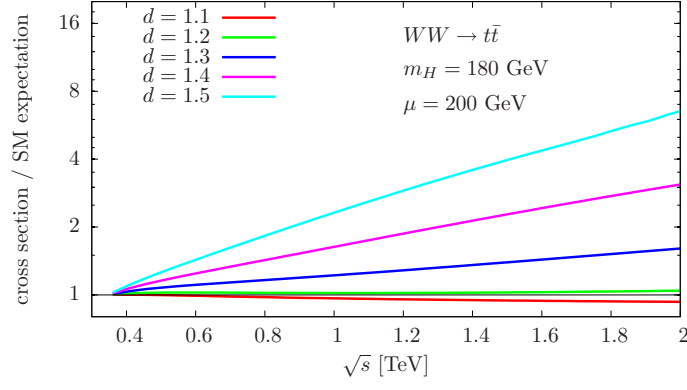


FIG. 3: The $W^+(m_W)W^-(m_W) \rightarrow t\bar{t}$ cross section for different values of the Unhiggs scaling dimensions d .

in the original paper is given by

$$\mathcal{L}_{Y,NC} = -\lambda_t \bar{t}_R \frac{H^\dagger}{\Lambda^{d-1}} \begin{pmatrix} t \\ b \end{pmatrix}_L + \text{h.c.} \quad (13)$$

where the “NC” stands for non-conformal. This Yukawa coupling is identical to that in the SM other than dividing by a power of the UV cutoff Λ which compensates for the fact that the Unhiggs doublet has dimension d instead of one. This leads to a coupling between the physical Unhiggs and $t\bar{t}$ given by

$$\Gamma_{Y,NC} = \frac{im_t}{v^d} \quad (14)$$

with

$$m_t = \frac{\lambda_t v^d}{\sqrt{2}\Lambda^{d-1}}. \quad (15)$$

The W^+W^-H vertex, when contracted with the polarization vectors, is given by [6]

$$ig^2 \Gamma^{+-\mu\nu} \varepsilon_\mu(k^-) \varepsilon_\nu(k^+) = i \frac{g^2 v^d}{2} \varepsilon(k^-) \cdot \varepsilon(k^+) \mathcal{K}(0, k^- + k^+) \quad (16)$$

where

$$\mathcal{K}(0, k^- + k^+) = -\frac{(\mu^2 - s)^{2-d} - (\mu^2)^{2-d}}{s} \quad (17)$$

and the Unhiggs propagator is given by

$$\Delta_H(s) = \frac{-i}{m^{4-2d} - \mu^{4-2d} + (\mu^2 - s)^{2-d}}. \quad (18)$$

Putting all of this together, the amplitude for the s -channel Unhiggs scattering (with helicities unspecified for now) is then given by

$$i\mathcal{M}_{H,NC} = ig^2 \bar{v}(p') \Gamma_Y u(p) \Delta_H(s) \Gamma^{+-\mu\nu} \varepsilon_\mu(k^-) \varepsilon_\nu(k^+) \quad (19)$$

where p and p' are the momenta of the incoming t and \bar{t} quarks respectively. After specifying the helicities (both right-handed) of the fermions and the polarizations (longitudinal) of the W s, we find that in the limit that $s \gg M_W^2, m_t^2$

$$\mathcal{M}_{H,NC} = -\sqrt{2} G_F m_t \sqrt{s} \left[\frac{\mu^{4-2d} - (\mu^2 - s)^{2-d}}{\mu^{4-2d} - m^{4-2d} - (\mu^2 - s)^{2-d}} \right]. \quad (20)$$

Finally we add this to the contribution to the amplitude from the other three diagrams given in Eq. (11) to get

$$\mathcal{M}_{NC} = -\sqrt{2} G_F m_t \sqrt{s} \frac{m^{4-2d}}{\mu^{4-2d} - \mu^{4-2d} - (\mu^2 - s)^{2-d}} \quad (21)$$

We can now safely take the limit $s \gg \mu^2, m^2$ which yields

$$\mathcal{M}_{NC} = \sqrt{2}G_F m_t m^{4-2d} (-1)^{d-2} s^{d-3/2} \quad (22)$$

The amplitude is an increasing function of s for $d > 1.5$, with the consequence that unitarity is not preserved in this process for $d \gtrsim 1.5$ (figure 3).

B. Elements of Unhiggs phenomenology at the LHC for $1 \leq d \leq 1.5$

In this section, we comment on the collider phenomenology that arises from the modified Yukawa and gauge sector of the Unhiggs model in the parameter range $1 \leq d \lesssim 1.5$. There are two sources of potential deviations of the Unhiggs scenario from SM-like production due to the underlying conformal structure of the symmetry breaking sector, which can be accessed in production processes of massive electroweak bosons [6]:

1. By eating a continuum Goldstone boson, the phase space of the longitudinal W receives a continuum contribution above the conformal symmetry breaking scale μ ,

$$d\Phi_W = 2\pi\theta(q^0)\delta(q^2 - m_W^2) + \theta(q^0)\theta(q^2 - \mu^2)f(q^2), \quad (23a)$$

where

$$f(q^2) = \frac{-2(2-d)\mu^{2-2d}\sin(\pi d)(q^2 - \mu^2)^{2-d}}{\mu^{8-4d} + (q^2 - \mu^2)^{4-2d} - 2\mu^{4-2d}\cos(\pi d)(q^2 - \mu^2)^{2-d}}. \quad (23b)$$

2. The Unhiggs, the W, Z propagators and the trilinear HZZ and HWW vertices are modified with respect to the SM, yielding, *e.g.*,

$$\frac{\sigma^{\text{Unh}}(gg \rightarrow H \rightarrow VV)}{\sigma^{\text{SM}}(gg \rightarrow H \rightarrow VV)} \sim \left| \left(1 - \frac{m_H^2}{q^2} \right) \frac{[(\mu^2 - q^2)^{2-d} - \mu^{4-2d}]}{(\mu^2 - q^2)^{2-d} - (\mu^2 - m_H^2)^{2-d}} \right|_{q^2=\sqrt{s}}^2, \quad (24)$$

where \sqrt{s} is the partonic center of mass energy as usual. Note that for $d = 1$ we have $\sigma^{\text{Unh}}/\sigma^{\text{SM}} = 1$.

We include both effects in figure 4, which compares $gg \rightarrow H \rightarrow W_L^+ W_L^-$ in the Unhiggs scenario and the Standard Model (SM) at the parton level for the typical scales which are probed at the LHC. We do not include the parton distribution functions at this point to make the comparison more transparent; comparing the main production mode contributing to the $pp \rightarrow VV + X$ cross sections at the LHC for Unhiggs and SM production, the gluon parton distribution have no phenomenological impact since they are identical. Integrating over the partonic energy fractions in computing the hadronic cross section, characteristics of comparison such as the dip for $\sqrt{s} \sim \mu$ are completely washed out.

The cross section qualitatively follows Eq. (24) with the continuum contributions of Eq. (23) ranging at the percent-level for fully-inclusive production. An important feature of Unhiggs production $pp \rightarrow H$ is that, with respect to the SM, the cross section decreases for scaling dimensions $d > 1$. This is a consequence of the Unhiggs' gauge interactions

$$\mathcal{L} \supset H^\dagger (D^\mu D_\mu + \mu^2)^{2-d} H, \quad (25)$$

where D_μ denotes the familiar $SU(2)_L \times U(1)_Y$ gauge covariant derivative. Consequently, the gauge interactions of the Unhiggs can be dialed away by increasing d while keeping the W and Z masses fixed. This can lead to a qualitatively different phenomenology compared to SM gluon fusion: the total Unhiggs cross section can remain small even if large corrections from strong interactions [22] are taken into account. At the same time, however, the Unhiggs branching ratios to massive gauge bosons decrease and, depending on the Higgs mass region, the Unhiggs can avoid the current LHC bounds [14, 16].

The phenomenology of longitudinal polarizations of the massive W s and Z s probes the mechanism of electroweak symmetry breaking and is generically buried in a much larger transversely-polarized V spectrum. The longitudinal polarizations can, in principle, be extracted by exploiting the V_L 's characteristic decay and radiation pattern. While these effects are well-investigated for weak boson fusion (WBF) [23] where they have motivated a central jet veto to enhance longitudinal over transverse polarizations [24], only recently in Ref. [25] similar concepts have been applied to final state jet correlations in the context of subjet analyses. In total, however, getting a handle on the longitudinal part of the massive weak bosons remains an experimentally as well as theoretically ambitious task at hadron colliders.

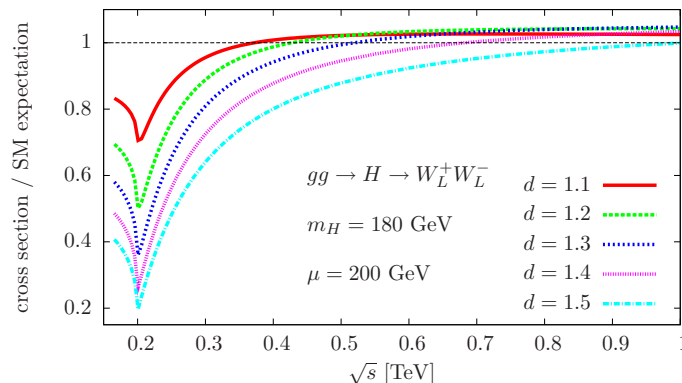


FIG. 4: Comparison of Unhiggs production and decay via gluon fusion, $gg \rightarrow H \rightarrow W^+W^-$ for different values of the Unhiggs scaling dimension $d \leq 1.5$ for identically chosen widths. \sqrt{s} denotes the partonic center of mass energy.

Applied to our case, the effect of Eq. (23) amounts to measuring a small excesses over the SM expectation in the invariant $V_L V_T, V_L V_L$ mass tails. Eventually, this becomes a hopeless endeavor at hadron colliders once theoretical and experimental systematic uncertainties of both the signal and the background of the order of a few percent are properly taken into account. Hence, in the actual experimental analysis, the focus is on reconstructing the unitarizing resonance mass. To dig out a resonance from a large continuous background we have to reconstruct the heavy gauge boson masses from their decay products. This is achieved by requiring the V decay product candidates to recombine the V mass within a certain mass window, which is essentially set by the experiment's resolution (see Refs. [26–28]). This eventually removes the reducible backgrounds to a large extent, but also the continuum contribution in Eq. (23) is excluded from the experimentally observed signal cross section due to the imposed selection criteria on either the fully-reconstructed invariant mass distribution or the transverse mass distribution of the partially-reconstructed final states (*e.g.* by projecting on events around the jacobian peak in the transverse cluster mass [24]).

As a consequence of the unitarization of the longitudinal VV ($V = W, Z$) scattering amplitudes as demonstrated in Ref. [6], the phenomenology of WBF processes [24, 29] remains unmodified over the entire parameter range in (d, μ, m_H) , except for the Higgs width modifications (see below). This directly follows from the comparison of the unpolarized $WW \rightarrow WW$ cross section in figure 5, where we plot the cross sections for identically chosen widths to make the comparison more transparent. Indeed the Unhiggs width does depend on the chosen values of d and μ (see below) but we will not discuss this in the context of WBF in more detail. Modified Higgs widths and the resulting modified cross sections with respect to the SM in WBF have been studied in *e.g.* Ref. [30].

The WW scattering cross section can be straightforwardly generalized to WBF with leptonic final states in the effective W approximation [31]. There is no quantitative modification when abandoning the effective W approximation

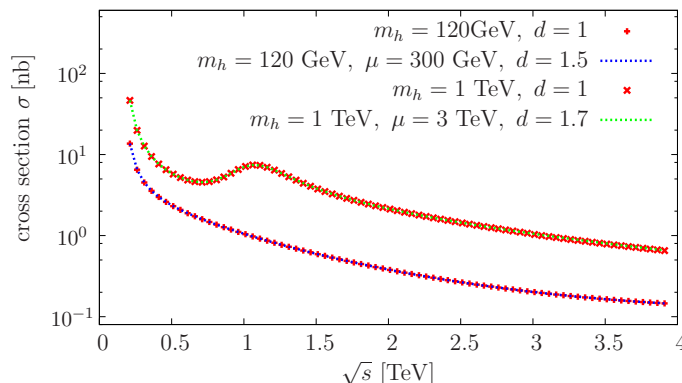


FIG. 5: Comparison of $W^+(m_W)W^-(m_W) \rightarrow W^+(m_W)W^-(m_W)$ cross section for Unhiggs production (lines) and in the SM (points and crosses). For comparison reasons we plot the cross section for identical widths. The cross section is to be understood as the double-pole part of the phase space integration Eq. (23), which reflects the experimental situation after reconstructing the final state W s.

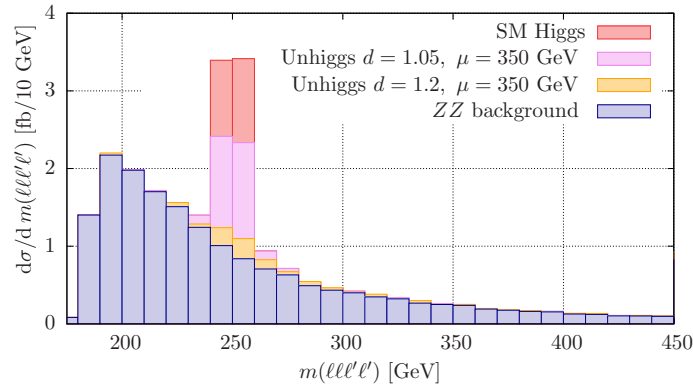


FIG. 6: Invariant four lepton mass in $pp \rightarrow ZZ + X \rightarrow 4\ell + X$ at the LHC ($\sqrt{s} = 14$ TeV) for the reconstruction requirements quoted in the text. We overlay the different signal hypotheses for comparison.

in favor of the full WBF matrix element in the Unhiggs scenario for, *e.g.* $pp \rightarrow 2j2\ell\cancel{E}_T$. The W, Z propagators in the Unhiggs model show modifications compared to the SM only in terms proportional to the four momentum, Eq. (1). Hence, potential modifications are parametrically suppressed by contracting the W, Z with light fermion currents in the full $2 \rightarrow 6$ WBF topologies [32]. This also accounts for the SM backgrounds to (Un)Higgs production.

Hence, we focus in the following on gluon fusion as production mode and consider decays $H \rightarrow VV$. This channel can be separated from WBF by imposing jet vetos. Nonetheless, since WBF phenomenology remains largely unmodified for $d > 1$ we can use the WBF channel to cross check the gluon fusion results and further constrain the Unhiggs scenario. Gluon fusion provides the largest production cross section for Higgs boson measurements at the LHC. Consequently, $gg \rightarrow H$ has received lots of attention from the phenomenology community (see *e.g.* Refs. [22, 33] for an overview). Along with the measurement of the Higgs branching ratios to massive gauge bosons, it provides a channel to study the interplay of the Yukawa and the gauge sectors*. This way we can experimentally infer deviations from the predicted SM rate, which naturally arise in the Unhiggs model.

As we will see, due to Eq. (25), putting stringent bounds on the Unhiggs parameters (d, μ, m_H) benefits from a clean environment and a very good background estimation. Quoting reliable confidence levels and discovery reaches therefore requires the inclusion of all contributing experimental uncertainties and $H \rightarrow ZZ$ provides a best-case channel to distinguish the SM Higgs from an Unhiggs. In order to minimize the impact of experimental systematics on our results we therefore investigate the mass regime $m_H \gtrsim 2m_Z$ with the Higgs decaying fully leptonically via two Z s in detail in this section. This so-called “gold-plated mode” offers the cleanest environment to study the Higgs sector’s anatomy, with only minimal impact of experimental uncertainties [34]. We note for completeness that Higgs properties can also be investigated with a boosted semi-hadronic final state [27]. The generalization of our results to fully leptonic WW and semi-hadronic WW and ZZ final states is straightforward.

In figure 6 we exemplarily compare the ZZ production (with leptonic decays) for SM Higgs and Unhiggs production for $m_H = 250$ GeV, $\mu = 350$ GeV, and $d = 1.05, 1.5$ and $d = 1.0$ (the SM Higgs). For details of the analysis see below. In this mass region, the LHC collaborations have become sensitive to SM-like cross sections recently [12] and we take this as an additional motivation to discuss the phenomenology that is implied by the Unhiggs scenario for the eventual high energy LHC run with a target luminosity of $\mathcal{L} \simeq 300 \text{ fb}^{-1}$ per experiment in this clean channel.

We adopt the fixed-width complex mass scheme [35] to model the Higgs width. For larger d and μ in Eq. (25), the Unhiggs decouples rapidly from the final state gauge boson’s phenomenology. At the same time the width decreases significantly for the chosen physical Unhiggs mass. With the mass of the W boson in the Unhiggs model [6] the width scales with respect to the SM Higgs boson width

$$\frac{\Gamma^{\text{Unh}}}{\Gamma^{\text{SM}}} \simeq \frac{(\mu^2)^{d-1}}{2-d} \left(\frac{(\mu^2)^{2-d} - (\mu^2 - m_H^2)^{2-d}}{m_H^2} \right)^2 \frac{-\pi \mathcal{A}_d}{2\pi \sin(\pi d)} \frac{(\mu^2 - m_H^2)^{d-1}}{2-d}, \quad (26)$$

**E.g.* by comparing to WBF as a purely electroweak production mode, which is also unaltered in our case, except for the modified Higgs width.

where

$$\mathcal{A}_d = \frac{16\pi^{5/2}}{(2\pi)^{2d}} \frac{\Gamma(d+1/2)}{\Gamma(d-1)\Gamma(2d)}. \quad (27)$$

Note that the Unhiggs width has mass dimension one for arbitrary values $1 \leq d < 2$, and we recover $\Gamma^{\text{Unh}}/\Gamma^{\text{SM}} = 1$ upon taking the limit $d \rightarrow 1$.

In fact, this is a very good approximation because we have $m_H < \mu$ in such a way that the W_L and Z_L boson can not access the continuum phase $q^2 \geq \mu^2$ in Eq. (23). Indeed a large μ for fixed d is preferred by electroweak precision constraints [10], however the phenomenology is largely independent of μ Eqs.(23),(24), (26). For the computation of figure 4 we found that the continuum leaves minor modifications in only the longitudinal components. Therefore, the above approximation should be sufficiently good to also govern the phenomenology for more general parameter choices if the WW and ZZ final states are the dominant Unhiggs decay channels. Furthermore, the total Higgs width is phenomenologically dominated by detector effects, and, hence, measurements of the absolute Higgs width are extremely involved at hadron colliders. In the clean $H \rightarrow ZZ \rightarrow 4\ell$, however the width is dominated by the physical one [12]. We note for completeness, that for smaller Unhiggs masses decays to fermions dominate, but also loop-induced decays can alter the Higgs phenomenology, especially for $d > 1.5$ when a modified fermion sector is realized. We leave a detailed investigation of this direction to future work.

For the purpose of this section, we are predominantly interested in assessing how and if the Unhiggs can be discriminated from the SM Higgs or the background. We adopt the viewpoint that d is a small quantity. This implies physics largely consistent with the SM to our current knowledge by construction. Consequently the branch cut of the Unhiggs phase space is subleading and the phenomenology is mainly affected by the modified Higgs resonance. We do not include signal-background interference effects with continuum $gg \rightarrow WW$ production [36], which will have an impact in high precision studies but will be of comparable size in both scenarios. We produce signal events with a modified version of MADEVENT [37] interfaced with HERWIG++ [38] and background events with SHERPA [39]. We require a minimum transverse momentum for four isolated leptons $p_T^\ell \geq 20$ GeV and a dilepton separation in the azimuthal angle-pseudorapidity plane $R_{\ell\ell'} \geq \sqrt{\Delta\eta_{\ell\ell'}^2 + \Delta\phi_{\ell\ell'}^2} \geq 0.2$. Throughout, we model finite detector resolution effects for leptons with a gaussian smearing by about

$$\frac{\Delta E}{E} = 0.02 \quad (28)$$

around the central true MC value, where E is the lepton's energy [40]. With an isolated lepton we mean an identified lepton in the electromagnetic calorimeter $|\eta| \leq 2.5$ with a hadronic energy deposit of smaller than 10% of the leptons' transverse momentum in a cone of size 0.3 around the lepton. The leptons are required to reconstruct the Z mass within a 10 GeV window with same flavor and opposite charge.

In the actual experimental analysis the normalization of the distributions in the theoretically challenged $pp \rightarrow VV$ production channel [41] is preferably extracted from data in control regions [12, 42]. The observed signal cross section is then a function of the background extrapolation. In order to be more realistic when testing the different hypothesis we conservatively account for higher order QCD corrections by including a total K -factor $K = 2$ for both signal and background[†]

We can already draw a few quantitative conclusion from figure 6. Measuring a SM Higgs-like excess in the considered mass range allows us to tightly constrain the (d, μ, m_H) parameter range already with low statistics. The smaller width at a lower physical Unhiggs production cross section leaves a narrow resonance which is washed out by detector and mass resolution effects. A precise determination of $d > 1$ for fixed μ and a statistically established resonance requires larger integrated luminosities. We discuss how this is quantitatively reflected in the full statistical analysis in the next section.

Hypothesis testing: Towards exclusion or discovery

To study these implications on a quantitative level we perform a log-likelihood shape comparison of the various hypotheses that are depicted figure 6. This is a standard method in the post-LEP era [44] which allows to compute confidence levels in a modified frequentist approach [45].

[†]It is known from the literature that $pp \rightarrow VV$ [41] receives large corrections $\mathcal{O}(50\%)$ at NLO QCD. NLO corrections to $pp \rightarrow VV + \text{jet}$ [43], which is a part of the NNLO VV production cross section is again large $\simeq 50\%$. The higher order corrections to Higgs production are also sizable [22]. In total higher order corrections have significant impact on our search.

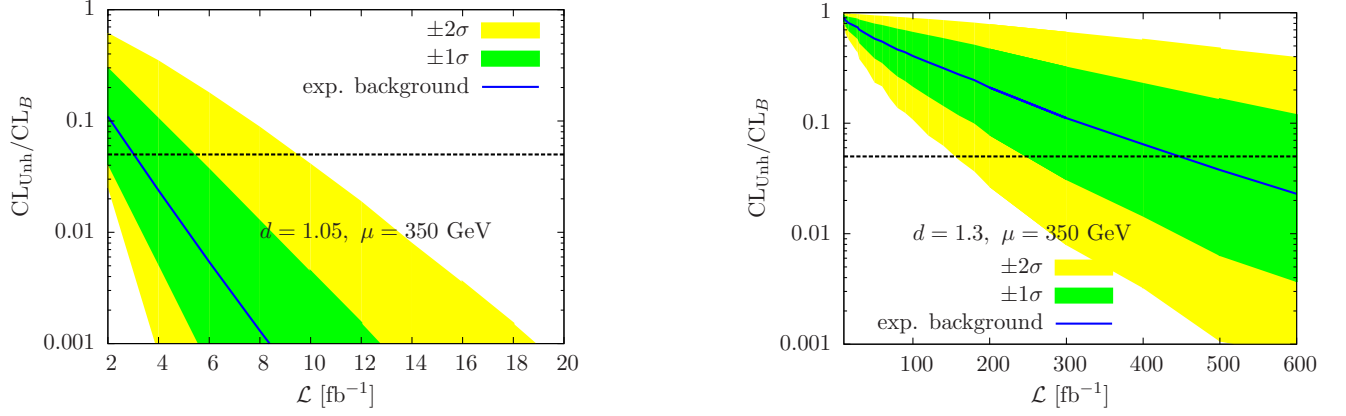


FIG. 7: Expected exclusion limit for the two Unhiggs benchmark points based on the given the background-only hypothesis for $\sqrt{s} = 14$ TeV at the LHC.

We define the log-likelihood ratio comparing the SM (null)hypothesis with the Unhiggs (alternative) hypothesis

$$Q = -2 \log \frac{L(\text{data} | \text{Unhiggs} + \text{background})}{L(\text{data} | \text{SM Higgs} + \text{background})}. \quad (29)$$

L denotes the Poissonian likelihood, *i.e.*

$$L(\text{data} | \text{Unhiggs} + \text{background}) = \frac{N^n e^{-N}}{n!}, \quad (30)$$

where $N = (\sigma^{\text{Unh}} + \sigma^{\text{bkg}})\mathcal{L}$ is the number of expected events at a given luminosity and n is the number of actually observed events in the Unhiggs model. Due to the additivity of the logarithm, the extension to differential distributions is straightforward. In the described scenario the log-likelihood picks up sensitivity from mostly around the Higgs peak, giving effectively rise to the comparison of counting experiments integrated over a few bins. Potential width-induced modifications of the phenomenology modulo detector and resolution effects are evidently incorporated in this approach.

According to the Neyman-Pearson lemma [46] Eq. (29) is the uniformly most powerful test statistic to discriminate between our two hypotheses (see Refs. [47, 48] for further details and phenomenological applications). We sample the two hypotheses with randomly generated pseudodata, yielding probability density functions (pdfs) $Q^{\text{Unh}}(Q)$ and $Q^{\text{SM}}(Q)$, for the Unhiggs and the SM distribution, respectively. From these pdfs we derive the confidence levels for exclusion and discovery. One main advantage of the log-likelihood hypothesis test is that there is a well-defined statistical notion for small luminosities which imply only a few bin counts. As already few bin entries can give rise to strong exclusion due to the large cross section deviations between the different hypotheses that are depicted in figure 6, this method yields reliable results, as opposed to significances $\sim \text{signal}/\sqrt{\text{background}}$, which are valid for large statistics.

Exclusion limits are conventionally expressed by computing the CL_S ratio [45], *i.e.*

$$\text{CL}_S = \frac{\text{CL}_{\text{Unh}}}{\widetilde{\text{CL}}_{\text{SM}}}. \quad (31)$$

Exemplary CL_S distributions as functions of the integrated luminosity are shown in figures 7 and 8 for $d = 1.05$, 1.3 , $m_H = 250$ GeV and $\mu = 350$ GeV. We also include the CL_S contours for the $\pm 1\sigma$ and $\pm 2\sigma$ edges of the respective null hypothesis as colored bands. These parameter choices are motivated by their preferred consistency with the SM Higgs+background and the background-only hypothesis, respectively.

The physics community refers to the parameter interval resulting from $\text{CL}_S \leq 0.05$ as “excluded at the 95% confidence level” by convention [45]; for $\text{CL}_S \leq 0.05$ the Unhiggs “false exclusion”

$$\text{CL}_{\text{Unh}} = \int_{\langle Q \rangle^{\text{SM}}}^{\infty} dQ Q^{\text{Unh}}(Q) \quad (32)$$

is smaller than 5% of the potential SM exclusion confidence level

$$\widetilde{\text{CL}}_{\text{SM}} = \int_{\langle Q \rangle^{\text{SM}}}^{\infty} dQ Q^{\text{SM}}(Q), \quad (33)$$

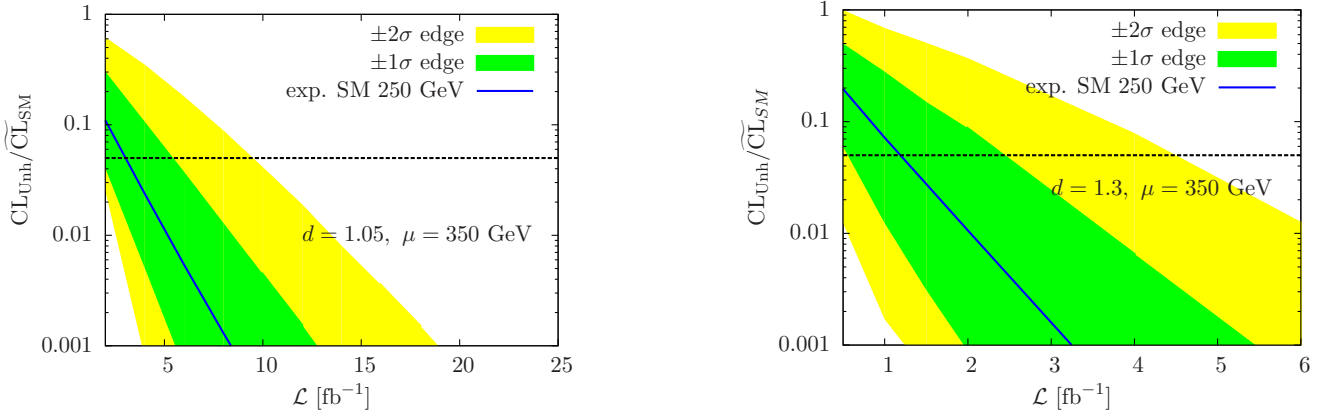


FIG. 8: Expected exclusion limit for the two Unhiggs benchmark points based on the given a SM-like Higgs excess null hypothesis for $\sqrt{s} = 14$ TeV at the LHC.

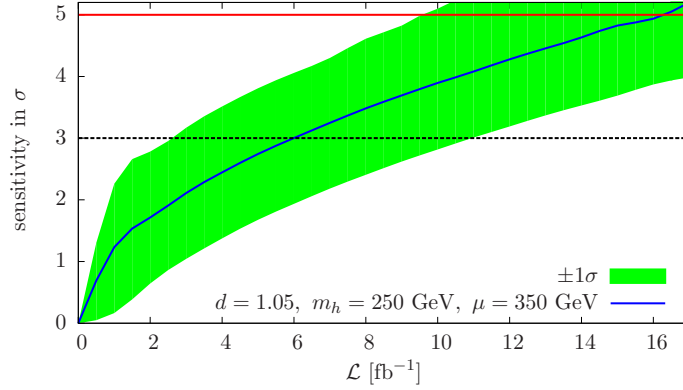


FIG. 9: Statistical significance of Unhiggs+background vs background-only as a function of the integrated luminosity for $d = 1.05$, $m_H = 250$ GeV, $\mu = 350$ GeV.

where $\langle Q \rangle$ denotes the median of the respective sampled pdf. figure 7 displays confidence levels of Unhiggs+background vs background-only, applying the identical approach. The expected alternative hypotheses' $CL_S = 0.5$ follows from Eqs. (32) and (33), accordingly.

Figures 7 and 8 deserve some comments. The central blue line gives CL_S as a function of the integrated luminosity, taking the Monte Carlo-generated data of figure 6 for the respective null hypothesis at face value (*i.e.* the expected value of CL_S). The shaded bands amount to the CL_S values within $\pm 1\sigma$ and $\pm 2\sigma$ fluctuations of the background distribution at the given integrated luminosity. If the null hypothesis is not disfavored, the observed CL_S value should fall within the shaded bands (see Ref. [14, 16] for the CL_S results of current SM Higgs searches.). Since CL_S is a ratio of confidence levels rather than a confidence level itself, its interpretation does not directly relate to the usual language of a 5σ discovery or exclusion. Instead it gives a conservative interpretation of the measured data, which is protected against insufficient statistics or insufficiently known backgrounds entering the measured likelihood ratio [45].

To estimate the luminosity at which we can expect the described Unhiggs scenarios to be eventually measured statistically significant, we identify the p value (which relates to the actually measured value Q by the experiment) with the median of the Unhiggs+background hypothesis $\langle Q \rangle^{\text{Unh}}$. This amounts to a situation when the experiment's outcome exactly follows the Unhiggs median, thus giving rise to a lower luminosity bound for discovery. We compute significances from the probability of the background-only hypothesis to yield a result compatible with the Unhiggs hypothesis by statistical fluctuations, *i.e.* we compute the “false discovery rate”

$$1 - CL_B = \int_{-\infty}^{\langle Q \rangle^{\text{Unh}}} dQ Q^B(Q). \quad (34)$$

A value of $1 - \text{CL}_B < 2.87 \times 10^{-7}$ corresponds to the familiar notion of a discovery with a significance of larger than 5σ . In figure 9, we also show the $\pm 1\sigma$ uncertainty band that arises from our computation of confidence levels.

Figures 7, 8 and 9 quantitatively confirm the statements at the end of the previous section. In general, for $d < 1.5$ the increasingly narrow resonance and the naive suppression of the $pp \rightarrow H$ cross section due to Eq. (25) leave a generically smaller cross section than expected in the SM. Consequently, the current exclusion bounds from the 7 TeV LHC data sample can be avoided. Also, if a SM-like Higgs excess is measured statistically significant in the near future, severe constraints on the combination of (d, μ) follow immediately.

Eventually abandoning the Unhiggs hypothesis in favor of the SM becomes a question of large integrated luminosity, and, more importantly, experimental systematics. Since for small $d > 1$ the Unhiggs quickly approaches the SM, the small differences in the cross section are difficult to access experimentally, given the residual uncertainty of the background. In this sense the considered channel is indeed a best-case scenario. Further discriminating the Unhiggs from the SM Higgs requires a detailed spectroscopy of the measured excess, which is performed best at a future linear e^+e^- collider [49]. From figure 8 we conclude that the LHC can potentially probe $d \lesssim 1.3$ level with its target luminosity. This is also the luminosity at which WBF provides an additional excellent search channel (see, *e.g.*, [29] for a detailed signal and background analysis in the context of the SM), where the (Un)Higgs resonance is established at the 5σ level.

III. THE “CONFORMAL” YUKAWA COUPLING: USING THE ADS/CFT CORRESPONDENCE

In the longitudinal W boson scattering process [6], the only interactions involving the Unhiggs were gauge interactions, which preserve the conformal invariance at high energies. With the conformal invariance intact, unitarity is manifest. The root of the unitarity problem with the fermionic scattering process is that with the original Yukawa coupling we have explicitly broken the conformal invariance by introducing the cutoff Λ . This was the simplest coupling to introduce, but unlike the case of the gauge-Unhiggs interactions, it does not preserve the conformal nature of the theory, which causes unitarity to fail. In the case of the gauge interactions, there is a simple guiding principle which allows us to exactly determine couplings that preserve the conformal nature of the theory. The Unhiggs kinetic term in the action is completely determined by conformal invariance, and simply gauging this action yields gauge interactions which respect this invariance. Similarly, we expect that if we can find a Yukawa coupling which respects the conformal invariance, the $t\bar{t} \rightarrow W_L^+ W_L^-$ process will also be unitary. Unlike the case of the gauge interactions, which simply involved gauging the conformally invariant kinetic term, we will have to make use of the AdS/CFT correspondence between fields in AdS_5 and 4D unparticle fields to find a Yukawa term which is conformal at high energies, as in [5]. In this section, we detail the derivation of this “conformal” Yukawa coupling and show that unlike the naive SM-like case above, it is a non-local derivative coupling, a fact which is crucial for preserving unitarity.

We will use the conformally flat AdS metric

$$ds^2 = \frac{R^2}{z^2} (\eta_{\mu\nu} dx^\mu dx^\nu - dz^2) \quad (35)$$

with a brane located at $z = \varepsilon$, which is equivalent to a UV cutoff $\Lambda = 1/\varepsilon$, and the space extending to infinity. We will take the limit $\varepsilon \rightarrow 0$ at the end of the calculation. The field content in our model consists of a scalar field and two Dirac fermions. The scalar field on the boundary will turn out to be the 4D unparticle field. We aim to calculate the Yukawa coupling between the unparticle and two fermion zero modes. The scalar action is

$$S_\phi = \frac{1}{2} \int dx dz \left(\frac{R}{z} \right)^3 \left(\partial_M \phi \partial^M \phi - \frac{m^2 R^2}{z^2} \phi^2 \right) \quad (36)$$

In the fermion sector, we introduce two Dirac fermions Ψ_L and Ψ_R written in terms of Weyl fermions as follows:

$$\Psi_L = \begin{pmatrix} \chi_L \\ \psi_L \end{pmatrix} \quad (37)$$

and

$$\Psi_R = \begin{pmatrix} \chi_R \\ \psi_R \end{pmatrix}. \quad (38)$$

The fermion action is given by

$$S_f = \int d^4x dz \left(\frac{R}{z} \right)^4 \left[-i\bar{\chi}_{L/R} \bar{\sigma}^\mu \partial_\mu \chi_{L/R} - i\psi_{L/R} \sigma^\mu \partial_\mu \bar{\psi}_{L/R} + \frac{1}{2} \left(\psi_{L/R} \overleftrightarrow{\partial}_z \chi_{L/R} - \bar{\chi}_{L/R} \overleftrightarrow{\partial}_z \bar{\psi}_{L/R} \right) + \frac{c_{L/R} + m_{L/R} z}{z} (\psi_{L/R} \chi_{L/R} + \bar{\chi}_{L/R} \bar{\psi}_{L/R}) \right], \quad (39)$$

where $c_{L/R}$ are the bulk masses and $m_{L/R}$ are the coefficients of the z -dependent mass terms, which will allow a subset of the fermions to have zero modes. The preceding fermion action is designed to make sure that we get two Weyl fermions which have zero modes in addition to continuum modes [50]. Finally, the Yukawa interaction between the scalar and fermions is given by

$$S_Y = \int d^4x dz \left(\frac{R}{z} \right)^5 \frac{\lambda_5}{2} \phi (\chi_L \psi_R + \chi_R \psi_L) + \text{h.c.} \quad (40)$$

where λ_5 is a Yukawa coupling of mass dimension $-1/2$.

A. Analysis of the scalar action

First, we analyze the scalar action in Eq. (36). Using $\partial_M \phi \partial^M \phi = \partial_\mu \partial^\mu \phi - \partial_z \phi \partial_z \phi$, we find that upon variation of the action the equation of motion for ϕ is

$$\partial_\mu \partial^\mu \phi - \partial_z^2 \phi + \frac{3}{z} \partial_z \phi + \frac{m^2 R^2}{z^2} \phi = 0. \quad (41)$$

Going to momentum space, our differential equation for ϕ (with 4-momentum p) becomes

$$\partial_z^2 \phi(p, z) - \frac{3}{z} \partial_z \phi(p, z) + p^2 \phi(p, z) - \frac{m^2 R^2}{z^2} \phi(p, z) = 0. \quad (42)$$

The solution to this equation is

$$\phi(p, z) = A z^2 [a J_\nu(pz) + b Y_\nu(pz)], \quad (43)$$

where $\nu = \sqrt{4 + m^2 R^2}$ and $p \equiv \sqrt{p^2}$. We will see that ν relates to the scaling dimension of the unparticle via the relation $d_2 = 2 - \nu$. The values a and b are determined by the boundary conditions in the IR, $z \rightarrow \infty$, and we will leave them undetermined, while the normalization constant A is determined by the boundary conditions (BCs) on the UV brane [5]. We will impose the UV boundary condition $\phi(p, \varepsilon) = \phi_0(p)$. This determines A , and the solution to $\phi(p, z)$ becomes

$$\phi(p, z) = \phi_0(p) \left(\frac{z}{\varepsilon} \right)^2 \frac{a J_\nu(pz) + b Y_\nu(pz)}{a J_\nu(p\varepsilon) + b Y_\nu(p\varepsilon)}. \quad (44)$$

Plugging Eq. (42) back into the scalar action and integrating by parts, we find that the integral over z reduces to a pure boundary term on the UV brane:

$$S_\phi = \frac{1}{2} \int \frac{d^4p}{(2\pi)^4} \left[- \left(\frac{R}{z} \right)^3 \phi(-p, z) \partial_z \phi(p, z) \right] \Big|_\varepsilon. \quad (45)$$

By definition, $\phi(-p, \varepsilon) = \phi_0(-p)$, so we must calculate only the term $\partial_z \phi(p, z)|_\varepsilon$. Also, we are interested in the range of scaling dimensions $1 \leq d_S < 2$, which means that ν is constrained to the range $0 < \nu \leq 1$. For these values of ν , $Y_\nu(p\varepsilon) \gg J_\nu(p\varepsilon)$ as $\varepsilon \rightarrow 0$. Therefore we will only need to keep the second term from the denominator of Eq. (44). Using these facts, and using the series expansions for the Bessel functions, we find that the action can be separated into a local term and a non-local term. The local term is given by

$$S_{\phi, (local)} = \frac{1}{2} \int \frac{d^4p}{(2\pi)^4} \phi_0(-p) \phi_0(p) \left(\frac{R}{\varepsilon} \right)^3 \left[\frac{-(2-\nu)}{\varepsilon} + \mathcal{O}(\varepsilon^0) \right]. \quad (46)$$

This local term can be removed by UV brane counterterms, and we will not consider them further [5]. The non-local term is given by

$$S_{\phi, (non-local)} = \frac{1}{2} \int \frac{d^4 p}{(2\pi)^4} \phi_0(-p) \phi(p) \left(\frac{R}{\varepsilon} \right)^3 \left[\frac{a}{b} \frac{\pi \varepsilon^{2\nu-1}}{2^{2\nu} [\Gamma(\nu)]^2} p^{2\nu} + \mathcal{O}(\varepsilon^{2\nu}) \right]. \quad (47)$$

If we rescale ϕ_0 so that

$$\phi'_0(p) = \phi_0(p) \left(\frac{R}{\varepsilon} \right)^{\frac{3}{2}} \sqrt{\frac{a}{b}} \frac{\sqrt{\pi} \varepsilon^{\nu-\frac{1}{2}}}{2^\nu \Gamma(\nu)} \quad (48)$$

we find that the non-local part of the action (in the $\varepsilon \rightarrow 0$ limit) is

$$S_{\phi, (non-local)} = \frac{1}{2} \int \frac{d^4 p}{(2\pi)^4} \phi'_0(-p) p^{2\nu} \phi'_0(p). \quad (49)$$

This action is exactly the action for a 4D scalar unparticle ϕ'_0 with scaling dimension $d_S = 2 - \nu$.

B. Analysis of the fermion action

We now proceed to solve for the 5D fermion wavefunctions from the action given in Eq. (39). From the variation of $\bar{\chi}_{L/R}$ we find

$$i\bar{\sigma}^\mu \partial_\mu \chi_{L/R} + \partial_z \bar{\psi}_{L/R} - \left(\frac{2 + c_{L/R}}{z} \right) \bar{\psi}_{L/R} - m_{L/R} \bar{\psi}_{L/R} = 0 \quad (50)$$

and from the variation of $\psi_{L/R}$ we find

$$i\sigma^\mu \partial_\mu \bar{\psi}_{L/R} - \partial_z \chi_{L/R} + \left(\frac{2 - c_{L/R}}{z} \right) \chi_{L/R} - m_{L/R} \chi_{L/R} = 0. \quad (51)$$

Next we separate the 5D fields as follows:

$$\chi_{L/R}(x, z) = \chi_{0,L/R}(x) g_{L/R}(z) \quad (52)$$

$$\bar{\psi}_{L/R}(x, z) = \bar{\psi}_{0,L/R}(x) h_{L/R}(z). \quad (53)$$

Using the 4D Dirac equations

$$i\bar{\sigma}^\mu \partial_\mu \chi_{0,L/R} = -p \bar{\psi}_{0,L/R} \quad (54)$$

$$i\sigma^\mu \partial_\mu \bar{\psi}_{0,L/R} = -p \chi_{0,L/R} \quad (55)$$

along with the fact that we are interested in zero modes ($p = 0$), we find the following equations for $g_{0,L/R}$ and $h_{0,L/R}$:

$$\partial_z g_{0,L/R} - \left(\frac{2 - c_{L/R}}{z} \right) g_{0,L/R} + m_{L/R} g_{0,L/R} = 0 \quad (56)$$

$$\partial_z h_{0,L/R} - \left(\frac{2 + c_{L/R}}{z} \right) h_{0,L/R} - m_{L/R} h_{0,L/R} = 0. \quad (57)$$

Solving for the zero mode wavefunctions, we get

$$g_{0,L/R}(z) = B_0 \left(\frac{z}{R} \right)^{2-c_{L/R}} e^{-m_{L/R} z} \quad (58)$$

$$h_{0,L/R}(z) = C_0 \left(\frac{z}{R} \right)^{2+c_{L/R}} e^{m_{L/R} z} \quad (59)$$

where B_0 and C_0 are normalization constants with mass dimension $1/2$. From the form of the zero mode solutions, we see that $\chi_{L/R}$ has a normalizable zero mode solution only for $m_{L/R} > 0$ while $\psi_{L/R}$ has a normalizable zero mode solution only for $m_{L/R} < 0$. We will choose $m_L > 0$ and $m_R < 0$, so that χ_L and ψ_R have zero modes,

whereas χ_R and ψ_L do not. The fermions will also have continuum modes (and possibly discrete modes with non-zero masses, depending on the values of $c_{L/R}$, see [50]) but we will only be interested in the zero modes for now. With the restriction that $m_L > 0$ and $m_R < 0$, the normalization constants are

$$B_0 = (2m_L R)^{-c_L} (2m_L)^{\frac{1}{2}} [\Gamma(1 - 2c_L, 2m_L \varepsilon)]^{-\frac{1}{2}} \quad (60)$$

$$C_0 = (-2m_L R)^{c_R} (-2m_R)^{\frac{1}{2}} [\Gamma(1 + 2c_R, -2m_R \varepsilon)]^{-\frac{1}{2}}. \quad (61)$$

For convenience, we define dimensionless normalization constants as follows:

$$B_0 = b_0 R^{-\frac{1}{2}} \quad (62)$$

$$C_0 = c_0 R^{-\frac{1}{2}}. \quad (63)$$

C. Analysis of the Yukawa coupling

We are now ready to calculate the form of the 4D Yukawa coupling between the scalar unparticle and the fermion zero modes. After Fourier transforming the 4D fermion fields, the first term in the Yukawa action (Eq. (40)) becomes

$$S_Y = \int \frac{d^4 q}{(2\pi)^4} \frac{d^4 k}{(2\pi)^4} \frac{d^4 p}{(2\pi)^4} \delta^4(p + q + k) dz \phi_0(p, z) \chi_{0,L}(k) \psi_{0,R}(q) \frac{\lambda_5}{\sqrt{2}} \left(\frac{R}{z}\right)^5 g_{0,L}(z) h_{0,R}(z). \quad (64)$$

Plugging in $\phi_0(p, z)$, $g_{0,L}(z)$ and $h_{0,R}(z)$ as well as substituting $\phi'_0(p)$ for $\phi_0(p)$, we find that the Yukawa coupling Γ_Y between the 4D fields $\phi'_0(p)$, $\chi_{0,L}(k)$ and $\psi_{0,R}(q)$ is given by

$$\Gamma_Y = \int dz \frac{\lambda_5}{\sqrt{2}} \left(\frac{\varepsilon}{R}\right)^{\frac{3}{2}} \sqrt{\frac{a}{b}} \frac{2^\nu \Gamma(\nu)}{\sqrt{\nu}} \frac{\varepsilon^{\frac{1}{2}}}{\varepsilon^\nu} \left(\frac{z}{\varepsilon}\right)^2 \frac{a J_\nu(pz)}{b Y(p\varepsilon)} B_0 C_0 \left(\frac{z}{R}\right)^{-1-c_L+c_R} e^{-(m_L-m_R)z} \quad (65)$$

and after taking $\varepsilon \rightarrow 0$ and simplifying we find

$$\Gamma_Y = -\frac{\gamma_5}{\sqrt{2}} \sqrt{\frac{a}{b}} R^{c_L-c_R-\frac{3}{2}} \sqrt{\pi} p^\nu b_0 c_0 \int z^{1-c_L-c_R} e^{-(m_L-m_R)z} J_\nu(pz) dz \quad (66)$$

where b_0 and c_0 are given in Eqs. (60)–(63). With an eye towards our later definition of the Yukawa coupling in the 4D theory, we redefine the conformal Yukawa coupling in Eq. (66) as

$$\Gamma_Y = -\frac{\lambda}{\Lambda^{d-1}} F(q^2) \quad (67)$$

where $F(p^2)$ encodes all of the momentum dependence and λ is a dimensionless coupling constant. To find $F(p^2)$, we must evaluate the integral over z in Eq. (66). It is given in [51]:

$$\int_0^\infty e^{-at} J_\nu(bt) t^{\mu-1} dt = \frac{\frac{1}{2} b^\nu \Gamma(\mu + \nu)}{(a^2 + b^2)^{\frac{1}{2}(\mu + \nu)} \Gamma(\nu + 1)} {}_2F_1\left(\frac{\mu + \nu}{2}, \frac{1 - \mu + \nu}{2}; \nu + 1; \frac{b^2}{b^2 + a^2}\right). \quad (68)$$

The above integral is convergent if the following conditions are met: $\text{Re}(a + ib) > 0$ and $\text{Re}(a - ib) > 0$ as well as $\text{Re}(\nu + \mu) > 0$. In our case, $b = p$, $a = m_L - m_R$ and $\mu = 2 - c_L + c_R$. Thus we see that for convergence $c_L - c_R < 2 + \nu$. Also, since p is always real, the only other condition is $m_L - m_R > 0$, which we already assumed to be true. Note that the limits of the above integral are zero to infinity as opposed to ranging from ε to infinity, which is the range of our integral over z in Eq. (66). This only introduces corrections of order ε , which will go to zero as we take $\varepsilon \rightarrow 0$. The Yukawa coupling then becomes

$$\begin{aligned} \Gamma_Y = & -\frac{\lambda}{\sqrt{2}} \sqrt{\frac{a}{b}} R^{c_L-c_R-1} \sqrt{\pi} p^\nu b_0 c_0 \frac{(\frac{1}{2}p)^\nu \Gamma(2 - c_L + c_R + \nu)}{((m_L - m_R)^2 + p^2)^{\frac{1}{2}(2 - c_L + c_R + \nu)} \Gamma(\nu + 1)} \\ & \times {}_2F_1\left(\frac{2 - c_L + c_R + \nu}{2}, \frac{c_L - c_R + \nu - 1}{2}; \nu + 1; \frac{p^2}{(m_L - m_R)^2 + p^2}\right). \end{aligned} \quad (69)$$

The conformal Yukawa coupling at high momentum

Since, to investigate unitarity, we are interested in the high energy behavior of the theory, we will want to take the high p limit of the conformal Yukawa coupling. In the limit $p \gg m_L - m_R$ the last argument of the hypergeometric function goes to one, allowing for considerable simplification. Substituting $\nu = 2 - d_S$, we get

$$\lim_{p \rightarrow \infty} \Gamma_Y = -\frac{\lambda}{\sqrt{2}} \sqrt{\frac{a}{b}} \frac{\pi}{2} b_0 c_0 \frac{\Gamma(2 - c_L + c_R + \nu)}{\Gamma\left(\frac{c_L - c_R + \nu}{2}\right) \Gamma\left(\frac{3 - c_L + c_R + \nu}{2}\right)} (pR)^{c_L - c_R - 1} p^{\nu - 1} \quad (70)$$

Making the fermions elementary

In the Unhiggs theory, we take the fermions to be elementary. Setting c_L and c_R to $1/2$ and $-1/2$ respectively yields a scaling dimension for the fermions of $3/2$, allowing for their interpretation as elementary. This yields the following form of the Yukawa coupling:

$$\lim_{p \rightarrow \infty, c_L=1/2, c_R=-1/2} \Gamma_Y = -\frac{\lambda}{\sqrt{2}} \sqrt{\frac{a}{b}} \frac{\pi}{2} b_0 c_0 \frac{\Gamma(3 - d)}{\Gamma\left(\frac{3-d}{2}\right) \Gamma\left(\frac{4-d}{2}\right)} p^{1-d}. \quad (71)$$

From now on we will take the Yukawa coupling with elementary fermions to be the definition of the Yukawa coupling in the Unhiggs theory. The important conclusion is that the momentum dependence of the coupling is simply p^{1-d} , so that

$$\lim_{p \rightarrow \infty} F(p^2) = A_d p^{1-d} \quad (72)$$

where A_d is a momentum-independent constant defined by Eqs. (67) and (71). We find then that the conformal coupling, unlike the non-conformal coupling, is a derivative coupling, depending on the momentum scale to a non-integer power.

D. Unitarity of $\bar{t}t \rightarrow W_L^+ W_L^-$ with the conformal coupling

Our previous calculation shows that the conformal Yukawa term in the Lagrangian is now given in momentum space by

$$L_{Y,C} = -\lambda_t \bar{t}_R \frac{H^\dagger(p)}{\Lambda^{d-1}} F(p^2) \begin{pmatrix} t \\ b \end{pmatrix}_L + \text{h.c.} \quad (73)$$

where $F(p^2)$ is given by $A_d p^{1-d}$ at high momentum. The mass term for the top quark is given by

$$m_t = \frac{\lambda_t v^d F(0)}{\sqrt{2} \Lambda^{d-1}}. \quad (74)$$

The value of $F(0)$ is arbitrary and for convenience we set it equal to 1, so that the mass term takes the same form as in the case with the non-conformal coupling (Eq. (14)). The Yukawa coupling between the physical Unhiggs and the $\bar{t}t$ pair is now given by

$$\Gamma_{Y,C} = i \frac{m_t}{v^d} F(p^2). \quad (75)$$

Therefore the Unhiggs exchange diagram will have a factor of $F(p^2)$ which was not present in the case of the non-conformal coupling.

There is another important consequence of the momentum dependence of the conformal Yukawa term in Eq. (73). Because it contains a derivative in position space, it must be gauged. Since it is non-local, it will yield terms in the Lagrangian coupling the Unhiggs, $\bar{t}t$ and arbitrary numbers of gauge bosons. More specifically, there will be a term in the Lagrangian coupling the Unhiggs, $\bar{t}t$ and two W bosons. Upon taking the Unhiggs to its VEV, this term will yield a contact interaction which will contribute to our scattering process $\bar{t}t \rightarrow W^+ W^-$. This diagram is shown in

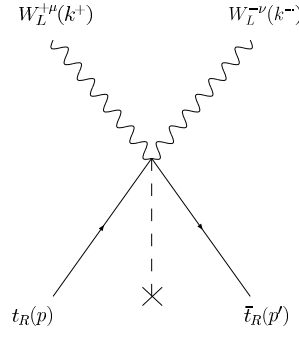


FIG. 10: The contact diagram which results from gauging the non-local Yukawa coupling. The cross denotes that the Unhiggs is taken to its VEV.

figure 10. We now proceed to derive the Feynman rule for this diagram. Using the result in [20], we find that after gauging Eq. (73), there is a term in the Lagrangian given by

$$\mathcal{L}_{Y,Gauge} = -g^2 \frac{\lambda}{\Lambda^{d-1}} \bar{t}_R H^\dagger(p) T^a T^b A_\alpha^a(q_1) A_\beta^b(q_2) \left(\begin{matrix} t \\ b \end{matrix} \right)_L G^{\alpha\beta}(p, q_1, q_2) + \text{h.c.} \quad (76)$$

where T^a, T^b are the generators for the gauge fields A_α^a, A_β^b and the function $G^{\alpha\beta}(p, q_1, q_2)$ is given by

$$G^{\alpha\beta}(p, q_1, q_2) = \frac{g^{\alpha\beta}}{2p \cdot (q_1 + q_2) + (q_1 + q_2)^2} [F((p + q_1 + q_2)^2) - F(p^2)] \quad (77)$$

$$+ \frac{(2p + q_2)^\beta [2(p + q_2) + q_1]^\alpha}{2(p + q_2) \cdot q_1 + q_1^2} \left[\frac{F((p + q_1 + q_2)^2) - F(p^2)}{2p \cdot (q_1 + q_2) + (q_1 + q_2)^2} - \frac{F((p + q_2)^2) - F(p^2)}{2p \cdot q_2 + q_2^2} \right] \quad (78)$$

Upon identifying the gauge bosons with W_μ^+ and W_μ^- (with momenta k^+ and k^- , respectively), this leads to a contact interaction between the top, anti-top and the two W bosons given by

$$ig^2 \Gamma_{Cont}^{+-\mu\nu} = i \frac{g^2}{2} \frac{\lambda_t}{\Lambda^{d-1}} \frac{v^d}{\sqrt{2}} G^{\mu\nu}(0, k^+, k^-) = \frac{-ig^2 m_t}{2} G^{\mu\nu}(0, k^+, k^-). \quad (79)$$

We now have two “Unhiggs” diagrams to consider: the first being the conformal Unhiggs s -channel exchange diagram in figure 2 and the second being the contact diagram in figure 10. The exchange diagram amplitude is simply given by the non-conformal amplitude from Eq. (20) multiplied by $F(s)$.

$$\mathcal{M}_{h,C} = -\sqrt{2} G_F m_t \sqrt{s} F(s) \left[\frac{\mu^{4-2d} - (\mu^2 - s)^{2-d}}{\mu^{4-2d} - m^{4-2d} - (\mu^2 - s)^{2-d}} \right] \quad (80)$$

The contribution to the amplitude from the contact diagram is given by

$$\mathcal{M}_{Cont} = \bar{v}(p') g^2 \Gamma_{Cont}^{+-\mu\nu} \varepsilon_\mu(k^+) \varepsilon_\nu(k^-) \quad (81)$$

which simplifies once we contract the vertex in Eq. (79) with the W polarization vectors. This yields

$$\varepsilon_\mu(k^+) \varepsilon_\nu(k^-) G^{\mu\nu}(0, k^+, k^-) = \varepsilon(k^+) \cdot \varepsilon(k^-) \frac{F(k^+ + k^-) - F(0)}{(k^+ + k^-)^2}. \quad (82)$$

Finally, putting the contributions from Eqs. (11), (80) and (83) together, the tree level amplitude for the process $\bar{t}t \rightarrow W_L^+ W_L^-$ is given by

$$\mathcal{M}_C = \sqrt{2} G_F m_t \sqrt{s} + \sqrt{2} G_F m_t \sqrt{s} [F(s) - 1] - \sqrt{2} G_F m_t \sqrt{s} F(s) \left[\frac{\mu^{4-2d} - (\mu^2 - s)^{2-d}}{\mu^{4-2d} - m^{4-2d} - (\mu^2 - s)^{2-d}} \right]. \quad (83)$$

Upon taking the limit $s \gg \mu, m^2$ this yields

$$\mathcal{M} = \sqrt{2} G_F m_t m^{4-2d} (-1)^{d-2} F(s) s^{d-\frac{3}{2}} \quad (84)$$

The only difference between this amplitude and the non-conformal amplitude is the presence of $F(s)$. This is a crucial difference, however, as upon taking the high energy limit of $F(s)$ we find that the amplitude becomes

$$\mathcal{M}_C = \sqrt{2}G_F m_t m^{4-2d} (-1)^{d-2} A_d s^{\frac{1-d}{2}} s^{d-\frac{3}{2}} = \sqrt{2}G_F m_t m^{4-2d} (-1)^{d-2} A_d s^{\frac{d-2}{2}} \quad (85)$$

We see that for all d in the range $1 \leq d < 2$ the amplitude is a decreasing function of s , and therefore the process does not violate unitarity.

IV. SUMMARY & CONCLUSION

The Unhiggs scenario [6] has interesting phenomenological implications, which can be tested at the LHC, already with early data [12, 52].

While spontaneous symmetry breaking assures that the weak boson fusion channels with clean leptonic final states remain unaltered, the unitarity bounds that result from the interplay of the Yukawa and gauge sector leave constraints on the model and imply a modified phenomenology of gluon fusion channels. We have investigated these modifications in the clean gold-plated mode $H \rightarrow ZZ \rightarrow 4$ leptons. Measurements in this clean channel will provide stringent bounds on the Unhiggs scenario, with only a minimum of experimental uncertainties. On the one hand, if a SM Higgs candidate in the mass range where this channel is important is observed in the future, we show that the Unhiggs hypothesis can in principle be tested at the percent-level in this channel. On the other hand the non-observation of Higgs can be accommodated in the Unhiggs scenario with $d \simeq 1.1$.

For $d > 1.5$ the low energy effective theory has to be completed by a conformally invariant Yukawa coupling to avoid unitarity violation in the massive quark scattering $\bar{t}t \rightarrow VV$ amplitudes. We achieve this by extending the $\bar{t}tH$ coupling of Ref. [6] to a “conformal” Yukawa coupling. Within the framework of AdS/CFT we demonstrate that this modified coupling serves to restore unitarity over the full parameter range $1 \leq d < 2$ in the high energy limit. This is tantamount to a modification of the heavy fermion sectors and an extended fermionic spectrum, and we leave a phenomenological analysis of these implications to future work.

Acknowledgements

C.E. and M.S. thank the physics department of the University of California, Davis, for hospitality. C.E. acknowledges funding by the Durham International Junior Research Fellowship scheme. J.T. was supported by the Department of Energy under grant DE-FG02-91ER406746.

-
- [1] H. Georgi, Phys. Rev. Lett. **98** (2007) 221601. [arXiv:hep-ph/0703260].
 - [2] H. Georgi, Phys. Lett. B **650**, 275 (2007). [arXiv:0704.2457 [hep-ph]].
 - [3] G. Cacciapaglia, G. Marandella and J. Terning, JHEP **0801** (2008) 070. [arXiv:0708.0005 [hep-ph]].
 - [4] P. J. Fox, A. Rajaraman and Y. Shirman, Phys. Rev. D **76** (2007) 075004. [arXiv:0705.3092 [hep-ph]].
 - [5] G. Cacciapaglia, G. Marandella and J. Terning, JHEP **0902**, 049 (2009). [arXiv:0804.0424 [hep-ph]].
 - [6] D. Stancato and J. Terning, JHEP **0911**, 101 (2009). [arXiv:0807.3961 [hep-ph]].
 - [7] A. Delgado, J. R. Espinosa, M. Quiros, JHEP **0710**, 094 (2007). [arXiv:0707.4309 [hep-ph]]. T. Kikuchi, N. Okada, Phys. Lett. **B661**, 360-364 (2008). [arXiv:0707.0893 [hep-ph]]. A. Delgado, J. R. Espinosa, J. M. No, M. Quiros, JHEP **0804**, 028 (2008). [arXiv:0802.2680 [hep-ph]]. A. Delgado, J. R. Espinosa, J. M. No, M. Quiros, JHEP **0811**, 071 (2008). [arXiv:0804.4574 [hep-ph]]. J. -P. Lee, [arXiv:0803.0833 [hep-ph]].
 - [8] J. R. Espinosa, J. F. Gunion, Phys. Rev. Lett. **82**, 1084-1087 (1999). [hep-ph/9807275]. J. J. van der Bij, S. Dilcher, Phys. Lett. **B655**, 183-184 (2007). [arXiv:0707.1817 [hep-ph]]. W. D. Goldberger, B. Grinstein, W. Skiba, Phys. Rev. Lett. **100**, 111802 (2008). [arXiv:0708.1463 [hep-ph]]. J. Fan, W. D. Goldberger, A. Ross, W. Skiba, Phys. Rev. **D79**, 035017 (2009). [arXiv:0803.2040 [hep-ph]].
 - [9] A. Falkowski, M. Perez-Victoria, Phys. Rev. **D79**, 035005 (2009). [arXiv:0810.4940 [hep-ph]]. A. Falkowski, M. Perez-Victoria, JHEP **0912**, 061 (2009). [arXiv:0901.3777 [hep-ph]].
 - [10] M. Beneke, P. Knechtges and A. Muck, JHEP **1110** (2011) 076 [arXiv:1108.1876 [hep-ph]].
 - [11] D. Stancato, J. Terning, Phys. Rev. **D81**, 115012 (2010). [arXiv:1002.1694 [hep-ph]].
 - [12] ATLAS collaboration, ATLAS-CONF-2011-131, arXiv:1202.1415 [hep-ex]. CMS collaboration, CMS-HIG-11-015, arXiv:1202.1997 [hep-ex].
 - [13] C. Englert, J. Jaeckel, E. Re and M. Spannowsky, arXiv:1111.1719 [hep-ph]. B. A. Dobrescu, G. D. Kribs and A. Martin, arXiv:1112.2208 [hep-ph].

- [14] ATLAS collaboration, ATLAS-CONF-2011-163.
- [15] ATLAS Collaboration, arXiv:1112.2577 [hep-ex], ATLAS-CONF-2011-162.
- [16] CMS collaboration, CMS-PAS-HIG-11-032.
- [17] CMS Collaboration, CMS-PAS-HIG-11-029, CMS-PAS-HIG-11-030, CMS-PAS-HIG-11-031.
- [18] C. Englert, T. Plehn, M. Rauch, D. Zerwas and P. M. Zerwas, Phys. Lett. B **707**, 512 (2012) [arXiv:1112.3007 [hep-ph]]. D. Carmi, A. Falkowski, E. Kuflik and T. Volansky, arXiv:1202.3144 [hep-ph]. A. Azatov, R. Contino and J. Galloway, arXiv:1202.3415 [hep-ph]. J. R. Espinosa, C. Grojean, M. Muhlleitner and M. Trott, arXiv:1202.3697 [hep-ph].
- [19] J. M. Maldacena, Adv. Theor. Math. Phys. **2**, 231 (1998) [Int. J. Theor. Phys. **38**, 1113 (1999)] [hep-th/9711200]. S. S. Gubser, I. R. Klebanov and A. M. Polyakov, Phys. Lett. B **428**, 105 (1998) [hep-th/9802109]. E. Witten, Adv. Theor. Math. Phys. **2**, 253 (1998) [hep-th/9802150].
- [20] S. Mandelstam, Annals Phys. **19**, 25 (1962). M. Chretien and R. E. Peierls, Proc. Roy. Soc. Lond. A **223**, 468 (1954) [World Sci. Ser. 20th Cent. Phys. **19**, 397 (1997)]. J. Terning, Phys. Rev. D **44** (1991) 887.
- [21] M. S. Chanowitz, M. A. Furman and I. Hinchliffe, Nucl. Phys. B **153**, 402 (1979).
- [22] H. M. Georgi, S. L. Glashow, M. E. Machacek and D. V. Nanopoulos, Phys. Rev. Lett. **40** (1978) 692D. A. Djouadi, M. Spira and P. M. Zerwas, Phys. Lett. B **264** (1991) 440. S. Dawson, Nucl. Phys. B **359**, 283 (1991). M. Spira, A. Djouadi, D. Graudenz and P. M. Zerwas, Nucl. Phys. B **453** (1995) 17 [arXiv:hep-ph/9504378]. R. V. Harlander and W. B. Kilgore, Phys. Rev. Lett. **88**, 201801 (2002) [hep-ph/0201206]. S. Catani, D. de Florian, M. Grazzini and P. Nason, JHEP **0307**, 028 (2003) [hep-ph/0306211]. S. Moch and A. Vogt, Phys. Lett. B **631**, 48 (2005) [hep-ph/0508265]. V. Ahrens, T. Becher, M. Neubert, L. L. Yang, Phys. Rev. D **79** (2009) 033013. [arXiv:0808.3008 [hep-ph]].
- [23] D. L. Rainwater, D. Zeppenfeld and K. Hagiwara, Phys. Rev. D **59**, 014037 (1998) [hep-ph/9808468]. N. Kauer, T. Plehn, D. L. Rainwater and D. Zeppenfeld, Phys. Lett. B **503**, 113 (2001) [hep-ph/0012351]. K. Arnold *et al.*, Comput. Phys. Commun. **180**, 1661 (2009) [arXiv:0811.4559 [hep-ph]] and arXiv:1107.4038 [hep-ph].
- [24] V. D. Barger, T. Han and J. Ohnemus, Phys. Rev. D **37** (1988) 1174. J. Bagger *et al.*, Phys. Rev. D **52** (1995) 3878. [arXiv:hep-ph/9504426].
- [25] T. Han, D. Krohn, L. T. Wang and W. Zhu, JHEP **1003** (2010) 082. [arXiv:0911.3656 [hep-ph]].
- [26] G. L. Bayatian *et al.* [CMS Collaboration], J. Phys. G **34** (2007) 995. G. Aad *et al.* [The ATLAS Collaboration], arXiv:0901.0512 [hep-ex].
- [27] C. Hackstein and M. Spannowsky, Phys. Rev. D **82** (2010) 113012. [arXiv:1008.2202 [hep-ph]]. C. Englert, C. Hackstein and M. Spannowsky, Phys. Rev. D **82** (2010) 114024. [arXiv:1010.0676 [hep-ph]].
- [28] M. H. Seymour, Z. Phys. C **62** (1994) 127. Y. Cui, Z. Han and M. D. Schwartz, Phys. Rev. D **83** (2011) 074023. [arXiv:1012.2077 [hep-ph]].
- [29] C. Englert, B. Jager, M. Worek and D. Zeppenfeld, Phys. Rev. D **80** (2009) 035027. [arXiv:0810.4861 [hep-ph]]. K. Doroba, J. Kalinowski, J. Kuczmarski, S. Pokorski, J. Rosiek, M. Szleper and S. Tkaczyk, arXiv:1201.2768 [hep-ph]. A. Ballestrero, D. Buarque Franzosi, L. Oggero and E. Maina, arXiv:1112.1171 [hep-ph].
- [30] S. Bock, R. Lafaye, T. Plehn, M. Rauch, D. Zerwas and P. M. Zerwas, Phys. Lett. B **694** (2010) 44 [arXiv:1007.2645 [hep-ph]]. C. Englert, T. Plehn, D. Zerwas and P. M. Zerwas, Phys. Lett. B **703** (2011) 298 [arXiv:1106.3097 [hep-ph]]. I. Low, P. Schwaller, G. Shaughnessy and C. E. M. Wagner, Phys. Rev. D **85**, 015009 (2012) [arXiv:1110.4405 [hep-ph]]. E. Weihs and J. Zurita, JHEP **1202**, 041 (2012) [arXiv:1110.5909 [hep-ph]]. A. Djouadi, O. Lebedev, Y. Mambrini and J. Quevillon, arXiv:1112.3299 [hep-ph].
- [31] S. Dawson, Nucl. Phys. B **249** (1985) 42.
- [32] B. Jager, C. Oleari and D. Zeppenfeld, JHEP **0607** (2006) 015. [arXiv:hep-ph/0603177] generalizing to C. Englert, B. Jager and D. Zeppenfeld, JHEP **0903** (2009) 060 [arXiv:0812.2564 [hep-ph]] for modifications in the electroweak sector.
- [33] A. Djouadi, Phys. Rept. **457**, 1 (2008). [arXiv:hep-ph/0503172].
- [34] J.-C. Chollet *et al.*, ATLAS note PHYS-NO-17 (1992). L. Poggioli, ATLAS Note PHYS-NO-066 (1995). D. Denegri, R. Kinnunen and G. Roullet, CMS-TN/93-101 (1993). I. Iashvili R. Kinnunen, A. Nikitenko and D. Denegri, CMS TN/95-076. D. Bommestam *et al.*, Note CMS TN-1995/018. C. Charlot, A. Nikitenko and I. Puljak, CMS TN/95-101. G. Martinez, E. Gross, G. Mikenberg and L. Zivkovic, ATLAS Note ATL-PHYS-2003-001 (2003).
- [35] U. Baur and D. Zeppenfeld, Phys. Rev. Lett. **75**, 1002 (1995) [hep-ph/9503344]. A. Denner, S. Dittmaier, M. Roth, and D. Wackeroth, Nucl. Phys. B **560** (1999), 33 [arXiv:hep-ph/9904472] C. Oleari and D. Zeppenfeld, Phys. Rev. D **69** (2004), 093004 [arXiv:hep-ph/0310156].
- [36] J. M. Campbell, R. K. Ellis and C. Williams, JHEP **1110**, 005 (2011) [arXiv:1107.5569 [hep-ph]].
- [37] J. Alwall *et al.*, JHEP **0709** (2007) 028. [arXiv:0706.2334].
- [38] S. Gieseke *et al.*, arXiv:1102.1672 [hep-ph].
- [39] T. Gleisberg, S. Hoeche, F. Krauss, M. Schonherr, S. Schumann, F. Siegert and J. Winter, JHEP **0902** (2009) 007. [arXiv:0811.4622 [hep-ph]]. S. Schumann, F. Krauss, JHEP **0803** (2008) 038. [arXiv:0709.1027 [hep-ph]]. S. Hoeche, F. Krauss, S. Schumann, F. Siegert, JHEP **0905** (2009) 053. [arXiv:0903.1219 [hep-ph]].
- [40] W. W. Armstrong *et al.* [ATLAS Collaboration], CERN-LHCC-94-43.
- [41] J. Ohnemus, Phys. Rev. D **44** (1991) 1403. J. Ohnemus, Phys. Rev. D **44** (1991) 3477. J. Ohnemus, Phys. Rev. D **47** (1993) 940. J. Ohnemus, J. F. Owens, Phys. Rev. D **43** (1991) 3626. J. Ohnemus, arXiv:hep-ph/9503389.
- [42] CMS collaboration, CMS PAS HIG-11-003.
- [43] V. Del Duca, F. Maltoni, Z. Nagy and Z. Trocsanyi, JHEP **0304** (2003) 059. [hep-ph/0303012]. S. Dittmaier, S. Kallweit and P. Uwer, Phys. Rev. Lett. **100**, 062003 (2008). [arXiv:0710.1577 [hep-ph]]. F. Campanario, C. Englert, M. Spannowsky and D. Zeppenfeld, Europhys. Lett. **88** (2009) 11001. [arXiv:0908.1638 [hep-ph]]. T. Binoth, T. Gleisberg, S. Karg, N. Kauer and G. Sanguinetti, Phys. Lett. B **683**, 154 (2010). [arXiv:0911.3181 [hep-ph]]. F. Campanario, C. Englert, S. Kallweit,

- M. Spannowsky and D. Zeppenfeld, JHEP **1007**, 076 (2010) [arXiv:1006.0390 [hep-ph]].
- [44] R. Barate *et al.* [LEP Working Group for Higgs boson searches], Phys. Lett. B **565** (2003) 61. [arXiv:hep-ex/0306033].
P. Bock *et al.* [ALEPH and DELPHI and L3 and OPAL Collaborations], CERN-EP/98-046.
- [45] A. L. Read, CERN-OPEN-2000-205. A. L. Read, J. Phys. G **G28** (2002) 2693-2704.
- [46] J. Neyman and E. S. Pearson, Philosophical Transactions of the Royal Society of London. Series A Vol. 231, (1933), pp. 289-337.
- [47] T. Junk, Nucl. Instrum. Meth. A **434** (1999) 435, [arXiv:hep-ex/9902006]. T. Junk, CDF Note 8128 [cdf/doc/statistics/public/8128]. T. Junk, CDF Note 7904 [cdf/doc/statistics/public/7904]. H. Hu and J. Nielsen, in 1st Workshop on Confidence Limits, CERN 2000-005 (2000) [arXiv:physics/9906010].
- [48] K. Cranmer and T. Plehn, Eur. Phys. J. C **51** (2007) 415 [arXiv:hep-ph/0605268]. D. E. Soper and M. Spannowsky, JHEP **1008** (2010) 029 [arXiv:1005.0417 [hep-ph]]. C. Englert, T. Plehn, P. Schichtel and S. Schumann, Phys. Rev. D **83** (2011) 095009 [arXiv:1102.4615 [hep-ph]].
- [49] G. Aarons *et al.* [ILC Collaboration], arXiv:0709.1893 [hep-ph]. J. A. Aguilar-Saavedra *et al.* [ECFA/DESY LC Physics Working Group Collaboration], hep-ph/0106315.
- [50] H. Cai, H. -C. Cheng, A. D. Medina, J. Terning, Phys. Rev. **D80**, 115009 (2009) [arXiv:0910.3925 [hep-ph]].
- [51] G.N. Watson, "Theory of Bessel Functions" University Press, Cambridge, 1952 (385).
- [52] C. Englert, D. Goncalves-Netto, M. Spannowsky and J. Terning, arXiv:1205.0836 [hep-ph].